Interference phenomena between two wave functions

Authors: Arnau Prat Pou
Facultat de Física, Universitat de Barcelona, Diagonal 645, 08028 Barcelona, Catalonia, Spain.

Advisor: Dr. Montserrat Guilleumas Morell
(Dated: June 12, 2019)

Abstract: The aim of this project is to study the interference produced by the collision of two wave functions. To analyze them, we will program a Crank-Nicolson method in order to solve the time-dependent Schrödinger equation and obtain the dynamics of a particle under any external potential. We will first check our Crank-Nicolson algorithm with some analytic cases before studying a non-analytic situation, with a barrier between both particles.

I. INTRODUCTION

Bose-Einstein condensates have been an interesting tool for studying quantum mechanic properties. One of these properties is the interference effect [1] [2]. In this project we will consider a non-interacting system as a first step to understand this phenomena.

We will program a Crank-Nicolson method in order to solve the time-dependent, unidimensional Schrödinger equation and study some properties of the wave function under different situations. We will then use these properties to create interference fringe and we will analyse them.

A. Theoretical framework

The wave function of a system of non-interacting particles, Ψ, is described by the Schrödinger equation. The dynamics in one dimension can be obtained by solving the time-dependent Schrödinger equation:

$$i\hbar\frac{\partial}{\partial t}\Psi(x,t) = \left[-\frac{\hbar^2}{2m}\frac{\partial^2}{\partial x^2} + V(x)\right]\Psi(x,t)\,, \qquad (1)$$

where m is the mass of the particle and $V(x)$ is the trapping potential. Since the Bose-Einstein condensates are usually confined in a harmonic trap, we will consider the following potential:

$$V(x) = \frac{1}{2}m\omega^2\,x^2\,, \qquad (2)$$

where ω is the trapping frequency that defines the harmonic oscillator units of length $x_0 = \sqrt{\hbar/m\omega}$, energy $\epsilon_0 = \hbar\omega$ and time $t_0 = 1/\omega$. From now on, we will use harmonic oscillator units. The dimensionless Schrödinger equation is:

$$i\frac{\partial}{\partial t}\Psi(x,t) = \left[-\frac{1}{2}\frac{\partial^2}{\partial x^2} + \frac{1}{2}x^2\right]\Psi(x,t)\,. \qquad (3)$$

The ground state can be obtained analytically, which is a centered gaussian wave function. As we are interested in study the dynamics, we will consider as an initial wave function:

$$\Psi(x,0) = \frac{1}{\sqrt{2\pi\sigma^2}}\exp\left[-\frac{(x-d)^2}{2\sigma^2}\right], \qquad (4)$$

where σ is the width of the gaussian and d is the displacement respect to the origin. The ground state corresponds to $\sigma = 1$ and $d = 0$.

B. Crank-Nicolson method

The dynamics of a Bose-Einstein condensate cannot be solved analytically, therefore we need a numerical method. In this project we will use the Crank-Nicolson method, which is a time implicit, finite difference method widely used to solve partial differential equations [3]. It approximates the second derivative at two different times, at t and $t + \Delta t$. Here, the discretized Schrödinger equation takes the following form:

$$\frac{\Psi_k^{j+1} - \Psi_k^j}{\Delta t} = i\frac{1}{2}\frac{1}{2}\left[\frac{\Psi_{k+1}^j + \Psi_{k-1}^j - 2\Psi_k^j}{\Delta x^2} + \frac{\Psi_{k+1}^{j+1} + \Psi_{k-1}^{j+1} - 2\Psi_k^{j+1}}{\Delta x^2} - \frac{1}{2}(iV_k\Psi_k^j + iV_k\Psi_k^{j+1})\right] \qquad (5)$$

where j corresponds to the time coordinate, k to the space coordinate, Δx the space step and Δt the time step.

It can be shown that Eq. (5) can be rewritten in a tri-diagonal matrix form by rearranging the terms. In this form, it is computationally easier to solve the equation. If we define $r = i\Delta t/2\Delta x^2$, A as a tri-diagonal matrix with $2(1+r) + iV(x)\Delta t$ at the main diagonal and $-r$ at the upper and lower diagonal, and B as another tri-diagonal matrix with $2(1-r) - iV(x)\Delta t$ at the main diagonal and r at the upper and lower diagonal, Eq. (5) can be simplified to

$$A\vec{\Psi}^{j+1} = B\vec{\Psi}^j\,. \qquad (6)$$

If we know the values of A, B and $\vec{\Psi}^j$, one can find the value of $\vec{\Psi}^{j+1}$. If we compute it N_t times, we obtain a time-evolution for any potentials.

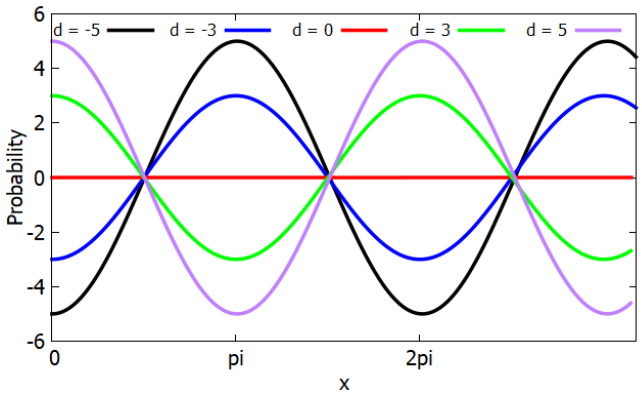

FIG. 1: Evolution of the expected value of the position, $< x >$, as a function of time for a displaced gaussian wave function under a harmonic trap in harmonic oscillator units.

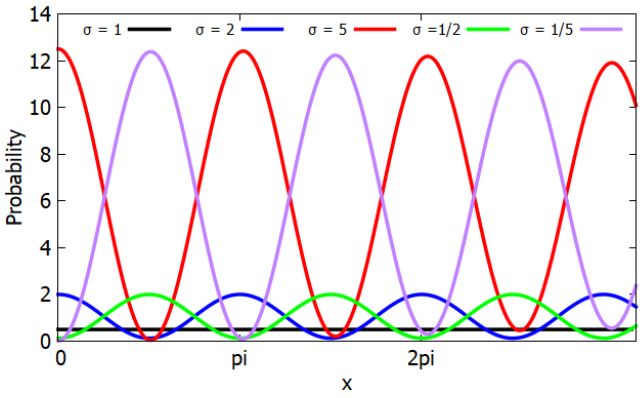

FIG. 2: Evolution of $< x^2 >$ as a function of time for a thinner or thicker gaussian wave function under a harmonic trap, in harmonic units.

II. EVOLUTION OF ONE PARTICLE

Before studying the collision of two wave functions, we will check the numerical code by studying the dynamics of an untrapped single particle and also in presence of a harmonic potential. We consider Eq. (4) as the initial wave function and we will numerically solve the dynamics by using the Crank-Nicolson method inside a box of length 100 (in harmonic units). The numerical parameters that we have used are $\Delta x = 0.05$ and $\Delta t = 0.01$.

A. Dipole mode

When the ground state of the harmonic potential is displaced from the center of the trap, it exhibits a periodic oscillation with the same frequency of the trap without changing the gaussian shape. This is the so called dipole mode.

We have obtained numerically the dipole oscillations by assuming as initial wave function Eq. (4) with $\sigma = 1$ and $d \neq 0$. In order to study them, we have computed the value of the expected value of the position, $< x >$ as a function of time. In Fig. 1 we can see the numerical results for different initial displacements. All the results follow the same equation:

$$< x >= d \cos(t)\,, \tag{7}$$

where t is the time in harmonic oscillator units. An interesting property of this result is that, independently of the initial separation, the period $T = 2\pi/\omega = 2\pi$ is always the same, sine the harmonic frequency ω does not change. The case $d = 0$ corresponds to a centered gaussian wave function, which is the stationary solution.

B. Breathing mode

Breathing mode occurs when a centred gaussian wave function has a width that does not correspond to the ground state of the harmonic potential. Therefore, we will aswell have as initial state a gaussian wave function with $\neq 0$ and $\sigma \neq 1$ confined in a harmonic trap.

In this situation, the wave function expands and contracts periodically. This is why, in this case, instead of computing and representing $< x >$, we will calculate $< x^2 >$ for $\sigma = 1, 2, 5, \frac{1}{2}$ and $\frac{1}{5}$. The numerical parameters are the same as in the dipole modes.

The numerical results are summarized in Fig. 2 As expected, $< x^2 > (t)$ shows a sinusoidal behaviour with the same period of $T = \pi$ in all the cases. It is also interesting to point out that the cases $\sigma = 2$ and $\sigma = 1/2$, or $\sigma = 5$ and $\sigma = 1/5$, have the same equation to describe $< x^2 >$ but with only a difference of a phase of π. During either the expansion or contraction, the width σ of the wave function becomes $1/\sigma$ in a time of $\pi/2$, the same periodic behaviour of $< x^2 > (t)$ but shifted.

C. Dispersion

The ground state of a harmonic potential, which consists of a gaussian wave function with $d = 0$ and $\sigma = 1$, does not evolve in time as we have checked numerically in Fig. 1 and 2 to test our computational code. However, if the trap is switched off, there will be a dispersion of the wave function. The probability can be calculated analytically:

$$|\Psi(x,t)|^2 = \frac{1}{\sqrt{\pi\,(1+t^2)}} \exp\left[-\frac{x^2}{(1+t^2)}\right]. \tag{8}$$

This equation describes the evolution of a free particle. Our wave function is trapped in a box of length 100. This will produce edge effects at large enough time, when the particle reaches the box limits. To avoid them, we will

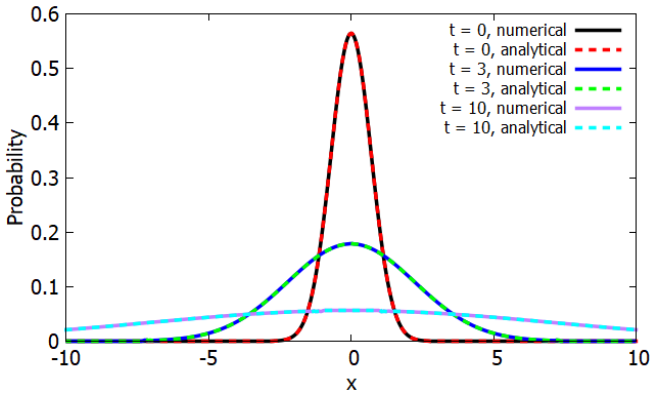

FIG. 3: Snapshots of the expansion of the wave function when the harmonic potential is switched off. The numerical results and the analytical ones, Eq. (8), are overlapped.

only study the dynamics from $t = 0$ to $t = 10$, when border effects are not relevant.

To study the validity of our Crank-Nicolson using Eq. (8), an animation sequence was created, plotting the analytical and numerical results. In Fig. 3 there are a few snapshots at different times. During all the time, the analytical and the numerical results are overlapped. Thus, showing an excellent agreement.

III. INTERFERENCE

Like a classical wave, when two coherent wave functions superpose, they produce interference phenomena. The fringes pattern depends on the initial separation, $2d$, and the relative phase between them, ϕ.

Experimentally, the interference pattern is produced by trapping two Bose-Einstein condensates in a double-well potential [1]. After switching off the trap, the condensates expand and when they overlap, the interference fringes appear. Another way to create interference is using the dipole mode, by trapping two particles at $\pm d$ in a harmonic potential. In this section we will study both ways and the effect of a potential barrier between the two wave functions.

A. Collision in presence of a harmonic potential

As we have seen before, in a harmonic potential, a gaussian wave function oscillates periodically with an amplitude of d, where d is the distance between the peak of the wave function and the center of the trap, and a period of $T = 2\pi$. That means that, if we displace two gaussian wave functions at $\pm d$, they will collide at $t = \frac{\pi}{2}$ and $x = 0$, forming an interference pattern.

We consider a wave function $\Psi(x,t)$ defined as

$$\Psi(x,t) = \Psi_l(x,t)e^{i\phi_l} + \Psi_r(x,t)e^{i\phi_r}\,, \tag{9}$$

where $\Psi_l(x,t)$ and $\Psi_r(x,t)$ will be our left and right gaussians wave functions, respectively, situated and $\pm d$, and ϕ_l and ϕ_r are they respective phases.

After this, we will normalize $\Psi(x,t)$ to 1 by computing $\int_{\infty}^{-\infty} |\Psi(x,t)|^2 dx = 1$ using the Simpsons rule.

Then, using the Crank-Nicolson method, we will obtain the numerical evolution of $\Psi(x,t)$. Since the Schrödinger equation is a linear equation, the result can be calculated analytically by computing

$$N|\Psi(x,t)|^2 = |\Psi_l(x,t)e^{i\phi_l} + \Psi_r(x,t)e^{i\phi_r}|^2\,, \tag{10}$$

where N is the normalisation constant. The obtained result, considering $\sigma = 1$, is the following one:

$$|\Psi(x, t = \pi/2)|^2 = Ne^{-x^2}\cos^2\left[\frac{1}{2}(2dx + \phi)\right]\,, \tag{11}$$

where $\phi = \phi_l - \phi_r$ is the relative phase and $t = \pi/2$ is the collision instant.

As we can see, the interference depend on the relative phase of both wave functions and the initial distance. The shape of the interference pattern will be a gaussian envelope and sinusoidal peaks. We can also see that, if we increase the initial distance, the peaks will be closer; and the phase difference will only add a phase to the peaks.

In Fig. 4 we show the snapshot of the numerical and analytical results at $t = \pi/2$ for two initial relative phases, $\phi = 0$ (top) and $\phi = \pi/2$ (bottom). The analytical results are overlapped with the numerical ones.

B. Collision in free space

In absence of a trapping potential, the wave functions expand. Due to the expansion, the wave functions will mix up, creating an interference pattern which will depend on the initial distance between them, $2d$, and their relative phase ϕ.

This pattern can also be found analytically. To calculate it, we can use Eq. (10) considering that the evolution of $\Psi(x,t)$ is described by Eq. (8). The final result is the following one [5]:

$$|\Psi(x,t)|^2 = \frac{N}{\sqrt{1+t^2}}\left[e^{-\frac{(x-d)^2}{(1+t^2)}} + e^{-\frac{(x+d)^2}{(1+t^2)}} + 2e^{-\frac{(x^2+d^2)}{(1+t^2)}}\cos\left(\frac{2dx}{t+1/t} + \phi\right)\right]. \tag{12}$$

The first two terms describe the expansion of the two wave functions, without considering the interaction between them, and it is consistent with Eq. (8). The third therm describes the interference pattern. We can see that, as before, it depends on the relative phase of both wave functions and its initial separation. There is also an additional time contribution, which did not appear in the harmonic potential. That contribution makes the envelope evolve like the wave function, and separates the

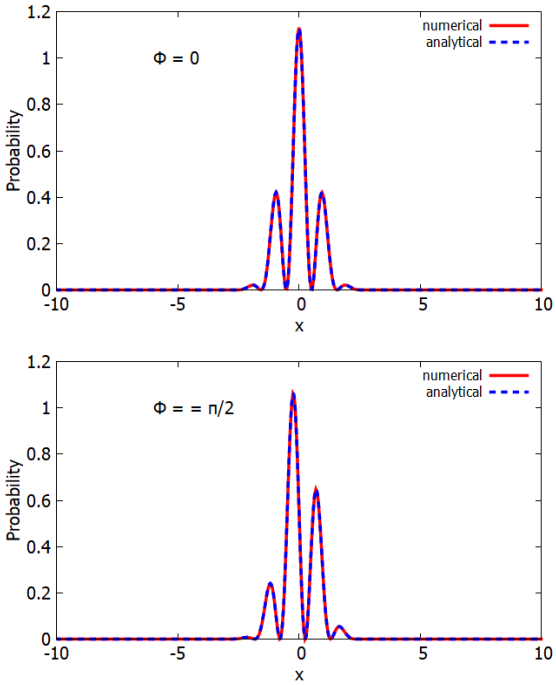

FIG. 4: Snapshot of the probability density at $t = \pi/2$ as a function of the position. The initial separation is $2d = 6$. Top panel corresponds to $\phi = 0$, and bottom panel to $\phi = \pi/2$. Numerical and analytical results are overlapped.

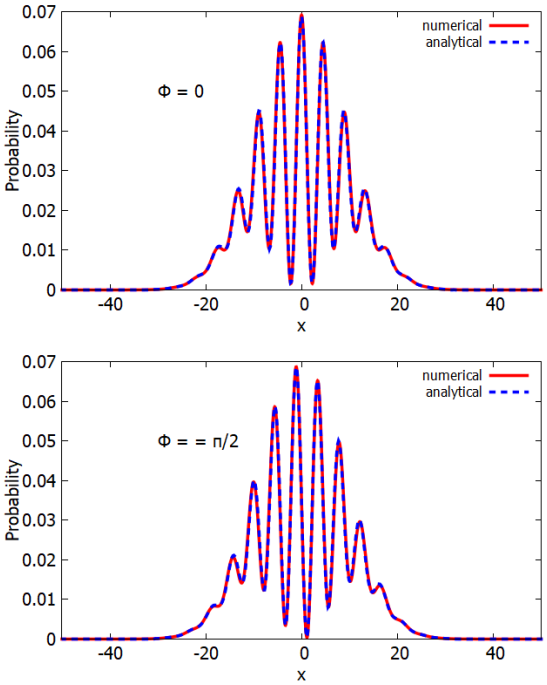

FIG. 5: Snapshot of the probability density at $t = 10$ as a function of the position. The initial separation is $2d = 14$. Top panel corresponds to $\phi = 0$, and bottom panel to $\phi = \pi/2$. Numerical and analytical results are overlapped.

peaks at large times. We can also see that, at small times, there will no be interference, since the wave functions will not have mixed yet.

We have obtained the dynamics by using the Crank-Nicolson method. Again, the numerical and analytical results are in agreement and they appear overlapped. Fig 5 shows two snapshots of the probability density at $t = 10$, with an initial separation $2d = 14$, and different relative phase, $\phi = 0$ (top panel) and $\phi = \pi/2$ (bottom panel).

C. Potential barrier effect

Let us consider a gaussian barrier centered in the harmonic potential,

$$V_{barrier}(x) = Ae^{-\frac{x^2}{2}}\,, \tag{13}$$

where A is the height of the gaussian potential. In this case, the total external potential will be

$$V(x) = \frac{1}{2}x^2 + V_{barrier}(x)\,. \tag{14}$$

The dynamic in this case cannot be solved analytically, so numerical results are needed to study it. We will consider three different cases affect the interference. To simplify the analysis, we will consider $\phi = 0$.

The first case we will consider is $A = 1$. Under this situation, the barrier potential will be almost negligible.

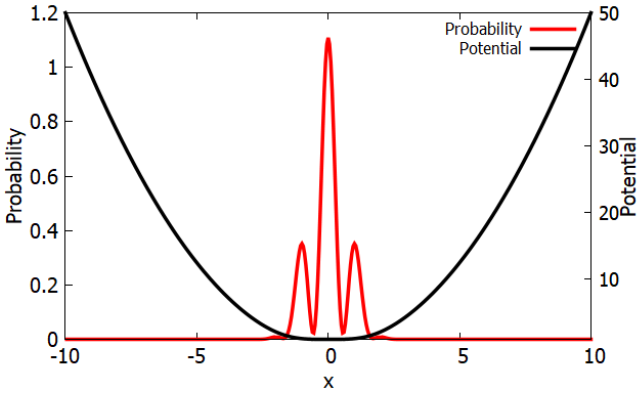

FIG. 6: Snapshot of the probability density at $t = \pi/2$ as a function of the position. The initial separation is $2d = 6$. Probability is represented in red and the potential in black.

To study how it affects, we will plot the density profile of the wave functions at the moment of the collision, which is $t = \pi/2$. Fig. 6 represents the snapshot of that instant. In it, we can see that the barrier is not strong enough to modify the interference.

Now we will consider a barrier of $A = 30$. In this case, the barrier is much stronger than the harmonic trap, so it will modify the interference pattern notably. To study it, we will plot the density profile at $t = \frac{\pi}{2}$, which is the collision frame, like in the previous case. The result is shown Fig. 7.

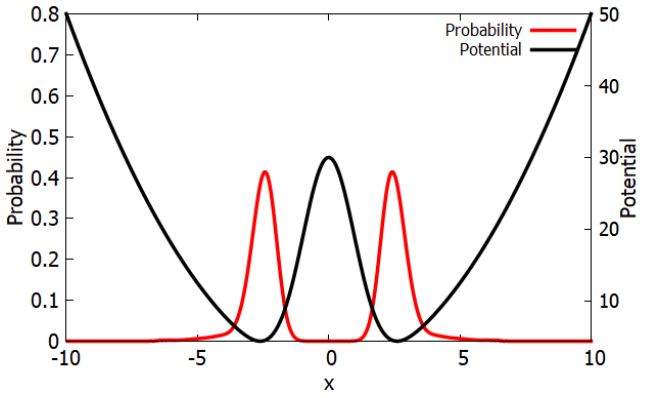

FIG. 7: Snapshot of the probability density at $t = \pi/2$ as a function of the position. The initial separation is $2d = 6$. Probability is represented in red and the potential in black.

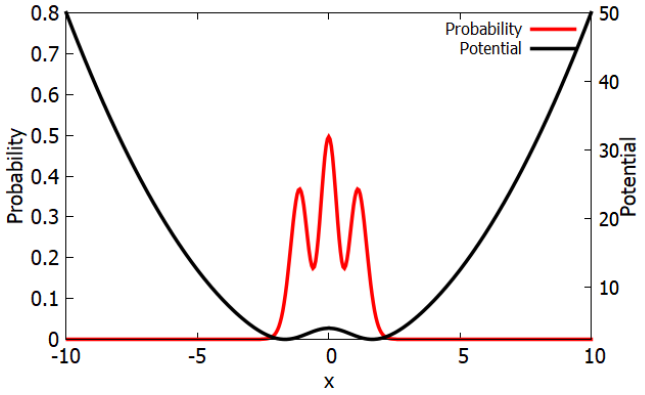

FIG. 8: Snapshot of the probability density at $t = \pi/2$ as a function of the position. The initial separation is $2d = 6$. Probability is represented in red and the potential in black.

As we can see, in this case the barrier is much stronger than the harmonic trap, so the wave functions stay in the minimal potential well. Because of that, there is no collision.

The last barrier potential we will study is the most interesting one, since the barrier is strong enough to modify the interference pattern, but not strong enough to stop the collision. This is the case of $A = 4$. As before, we will proceed to plot the density profile at $t = \frac{\pi}{2}$ to study the interference pattern. The results are summarized in Fig. 8. As we can see, the interference are shown, and the pattern is the same of Fig. 4, but they are clearly deformed if we compare them with the case without barrier.

IV. CONCLUSIONS

We have investigated the interference produced by the collision of two wave functions. We have constructed a numerical code to solve the time-dependent Schrödinger equation by mean of the Crank-Nicolson numerical method. We have used it to study the dynamic of a gaussian wave function under a harmonic trap and without external potential. By comparing our numerical results with the analytical predictions, we have checked the validity of our program.

We have then studied the interference produced by two wave functions in a few analytical and non-analytical cases.

An interesting next step would be to study a more realistic Bose-Einstein condensate, by adding the interaction term, and comparing those results with the ones obtained in this project to understand the role of interactions in the interference phenomena.

Acknowledgments

I would like to thank Dr. Montserrat Guilleumas and Dr. Bruno Juliá, who advised me during all the project and helped me creating the program used to do all the simulations.

[1] M. R. Andrews, C. G. Townsend, H.-J. Miesner, D. S. Durfee, D. M. Kurn and W. Ketterle. (1997). *Observation of Interference Between Two Bose Condensates*. Science 275 (5300), 637-641.

[2] K. B. Davis, M.-O. Mewes, M. R. Andrews, N. J. van Druten, D. S. Durfee, D. M. Kurn, and W. Ketterle. (1997). *Bose-Einstein Condensation in a Gas of Sodium Atoms*. Physiscal review lerrers, volume 75, number 22.

[3] Juliá Díaz, Bruno.(2017). *Física Computacional*.

[4] L. P. Pitaevskii, S. Stringari. (1993). *Theory of Bose-Einstein condensation in trapped gases*. Reviews of Modern Physics, Vol. 71, No. 3.

[5] H. Wallis, A. Röhrl, M. Naraschewski, A. Schenzle H. J. Miesner (1997). *Coherence of bose condensates*, Journal of Modern Optics, 44:10, 1751-1762

[6] A. Röhrl, M. Naraschewski, A. Schenzle, and H. Wallis. *Transition from Phase Locking to the Interference of Independent Bose Condensates: Theory versus Experiment*. Physiscal review lerrers, volume 78, number 22.

[7] E. Cornell. *Very Cold Indeed: The Nanokelvin Physics of Bose-Einstein Condensation*. Journal of Research of the National Institute of Standards and Technology.